Journal of Magnetic Resonance **141,** 180–184 (1999)
Article ID jmre.1999.1891, available online at http://www.idealibrary.com on IDEAL®

COMMUNICATIONS

Transverse-Relaxation-Optimized (TROSY) Gradient-Enhanced Triple-Resonance NMR Spectroscopy

J. Patrick Loria,* Mark Rance,† and Arthur G. Palmer, III*,[1]

*Department of Biochemistry and Molecular Biophysics, Columbia University, 630 West 168th Street, New York, New York 10032; and †Department of Molecular Genetics, Biochemistry, and Microbiology, University of Cincinnati, Cincinnati, Ohio 45267

Received April 7, 1999

Two modifications to sensitivity-enhanced gradient-selected TROSY-based triple-resonance NMR experiments are proposed that reduce the overall duration of the pulse sequences and minimize radiation damping effects on water-flipback solvent suppression. The modifications are illustrated for the HNCO–TROSY experiment, but are applicable to all triple-resonance experiments that detect proton magnetization after a reverse polarization transfer step from a ^{15}N spin. The methods are applied to yeast triosephosphate isomerase, a symmetric dimer with 248 amino acid residues per monomer.

Key Words: **TROSY; triple-resonance NMR spectroscopy; triosephosphate isomerase; gradient coherence selection.**

Transverse-relaxation-optimized spectroscopy (TROSY) recently has been introduced by Pervushin *et al.* (*1*) as a new approach for obtaining ^{1}H–*X* correlation spectra that utilizes the interference between the ^{1}H–*X* dipolar and the ^{1}H or *X* CSA relaxation mechanisms (*2*) to reduce resonance linewidths in multidimensional NMR experiments. The initial descriptions of the TROSY experiment for backbone ^{1}H–^{15}N correlations (*1*) and aromatic ^{1}H–^{13}C correlations (*3*) in proteins were quickly followed by extensions to triple-resonance NMR spectroscopy (*4*, *5*). The physical basis of the TROSY experiment and the sensitivity gains expected in double- and triple-resonance NMR spectroscopy have been analyzed elsewhere (*1*, *3*, *4*, *6*–*8*). The present Communication demonstrates modifications to sensitivity-enhanced, gradient-selected, triple-resonance TROSY experiments that reduce the duration of the pulse sequences to minimize relaxation losses and minimize radiation damping effects in water-flipback solvent suppression schemes. The modifications are illustrated for the HNCO–TROSY experiment, but are equally applicable to other double- and triple-resonance NMR experiments.

A conventional sensitivity-enhanced gradient-selected HNCO–TROSY pulse sequence is illustrated in Fig. 1a. The sequence is obtained by replacing the sensitivity-enhanced gradient-selected reverse polarization transfer step of a conventional HNCO experiment (*9*) with a sensitivity-enhanced gradient-selected TROSY sequence. The sequence differs from a phase-cycled HNCO–TROSY experiment (*4*) by the inclusion of the coherence selection gradients G3 and G6 and modification of the phase cycle. As shown, the sequence is extended by a short spin–echo period, τ–180°–τ, in order to incorporate the decoding gradient G6, as proposed in other gradient-selected TROSY experiments (*10*, *6*). As a result, the water ^{1}H magnetization is inverted along the $-z$ axis for the time period $\Delta + \tau$ prior to the last ^{1}H 180° pulse, which serves to return the water magnetization to $+z$ axis prior to the detection period. As has been discussed elsewhere (*11*) rapid radiation damping of the solvent signal at high static magnetic field strengths compromises water-flipback solvent suppression methods that must invert the water magnetization relative to methods that use crafted pulses to leave the water magnetization unperturbed along the $+z$ axis.

The modified HNCO–TROSY pulse sequence is illustrated in Fig. 1b. Two changes are incorporated into this experiment. First, a ^{13}CO 180° pulse (point a, Fig. 1b) is introduced to allow the ^{15}N–^{13}CO scalar coupling interaction to evolve during the first 2Δ period of the TROSY sequence element. Consequently, the ^{15}N constant time evolution period can be reduced to $\delta = T - 2\Delta$ and the overall duration of the experiment is reduced by 2Δ. Interference between the dipolar and CSA relaxation mechanisms, which forms the basis of the TROSY experiment, does not affect conformational exchange broadening of resonance signals. Thus, loss of signal intensity from exchange broadening is just as significant in TROSY-based experiments as in conventional heteronuclear correlation experiments and minimizing the overall length of the experiments is equally important. Second, the last half of the TROSY sequence element is modified to eliminate the need for the final ^{1}H 180° pulse in Fig. 1a. The 180° pulse depicted as an open rectangle in Fig. 1b is a selective or crafted pulse that leaves the water

[1] To whom correspondence should be addressed. Fax: (212) 305-7932; E-mail: agp6@columbia.edu.

1090-7807/99 $30.00

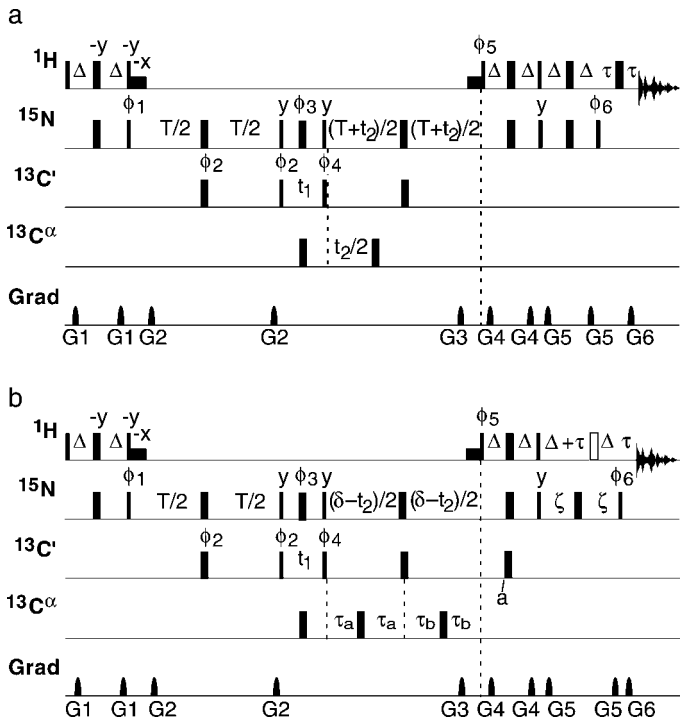

FIG. 1. Pulse sequences for HNCO–TROSY experiments. (a) Conventional sensitivity-enhanced gradient-selected HNCO–TROSY experiment. (b) Modified sensitivity-enhanced gradient-selected HNCO–TROSY experiment. All pulses are applied with x-phase unless otherwise indicated. Narrow and wide filled rectangles correspond to 90° and 180° rectangular pulses, respectively. The ^{1}H pulses are applied at the frequency of the H_2O resonance with $\gamma B_1 = 25$ kHz. Nitrogen pulses are applied at an offset of 120 ppm with $\gamma B_1 = 6.40$ kHz. The ^{13}CO pulses are applied at an offset of 173 ppm with $\gamma B_1 = \nu\sqrt{15} = 4.63$ kHz and the $^{13}C_\alpha$ pulses are applied at an offset of 55 ppm with $\gamma B_1 = \nu\sqrt{3} = 10.2$ kHz in which ν is the frequency difference between the ^{13}CO and $^{13}C_\alpha$ carriers. The filled squares are low power ^{1}H 90° pulses for water-flipback. In the present application, these were 1.4 ms rectangular pulses. The unfilled rectangle represents a crafted 180° inversion pulse that leaves the water magnetization unperturbed. In the present application, the 3-9-19 pulse was utilized (*13*). The delays are $\Delta = 2.75$ ms, $T = 22$ ms, $\delta = T - 2\Delta$, $\tau_a = (\delta - t_2)/4$, $\tau_b = (\delta + t_2)/4$, $\zeta = (\Delta + \tau/2)$, and $\tau = 250$ μs. The phase cycle is $\phi_1 = (x, -x)$, $\phi_2 = (x, x, -x, -x)$, $\phi_3 = (x, x, x, x, -x, -x, -x, -x)$, $\phi_4 = 308°$ to compensate for the off-resonance effects of the $^{13}C_\alpha$ 180° pulse during t_1, $\phi_5 = y$, $\phi_6 = x$, receiver = $(x, -x, -x, x)$. Gradient pulse lengths and strengths are $G1_z = (520\ \mu s, 6$ G/cm), $G2_z = (600\ \mu s, 4.8$ G/cm), $G3_{xyz} = (1.5$ ms, 24 G/cm), $G4_z = (500\ \mu s, 7.2$ G/cm), $G5_z = (500\ \mu s, 12$ G/cm), $G6_{xyz} = (150\ \mu s, 24.24$ G/cm). The gradient pulses have the shape of the center lobe of a sine function. Quadrature detection in t_1 is achieved by shifting ϕ_2 and the receiver following the States–TPPI protocol (*22*). PEP echo/antiecho coherence selection during t_2 (*23–25*) is obtained by inverting the sign of the gradient G6 and of pulse phases ϕ_5 and ϕ_6; ϕ_1 and the receiver were inverted on alternating t_2 increments. A sensitivity-enhanced, non-gradient-selected version of the pulse sequence of Fig. 1b is obtained by eliminating G3 and G6, setting $\tau = 0$, and utilizing the sensitivity-enhanced TROSY phase cycle (*14*).

magnetization along the $+z$ axis. Thus, the drawbacks associated with inverting the solvent magnetization in existing gradient-selected TROSY experiments are avoided. This modification to the TROSY refocusing period has been used previously by Dingley and Grzesiek in the quantitative HNN–COSY experiment (*12*). Most importantly, the advantages conferred by the modified pulse sequence are not accompanied by any significant ancillary drawbacks; consequently, these modifications are generally applicable.

The proposed modifications to the HNCO–TROSY experiment were tested on a [99%-^{13}C, 99%-^{15}N, 80%-^{2}H]-labeled W90Y, W157F mutant of yeast triosephosphate isomerase (TIM), a symmetric dimer (total $M_w = 54$ kD) with 248 amino acid residues per monomer. Preparation of the isotopically enriched protein is described elsewhere (*14*). The sample used for NMR spectroscopy was 0.9 mM (pH 5.9, 10 mM CD_3CO_2Na, 1 mM DTT, 0.02% NaN_3, 90%H_2O/10%D_2O). The experiment was performed on a Bruker DRX600 NMR spectrometer equipped with a three-axis gradient triple-resonance probe. The sample temperature was 293 K. The spectrum was recorded using a total of 16 transients per echo/antiecho pair, 64 × 32 × 1024 complex points and spectral widths of 2500 × 2500 × 10,000 Hz in F1(^{13}CO) × F2(^{15}N) × F3(^{1}H), respectively. The total acquisition time was 35 h. The spectrum was processed using Felix (Molecular Simulations, Inc.) and in-house FORTRAN programs by the PEP echo/antiecho procedure (*15*). A convolution filter was applied to the free-induction decays to suppress residual solvent signals (*16*). The FIDs were apodized with a 8 Hz exponential window function, zero-filled by a factor of two, Fourier transformed, and baseline corrected with a second-order polynomial function. The interferograms in the indirect dimensions were apodized using Kaiser window functions, zero-filled by a factor of two, and Fourier transformed.

To illustrate the quality of the data achievable using the TROSY approach in triple-resonance NMR experiments, one of the most crowded F1(^{13}CO) × F3(^{1}H) planes in the HNCO spectrum is shown in Fig. 2. The sensitivity gains afforded by TROSY-based triple resonance experiments have been discussed elsewhere (*4*). In accordance with these expectations, the TROSY–HNCO for TIM is approximately a factor of 2.5

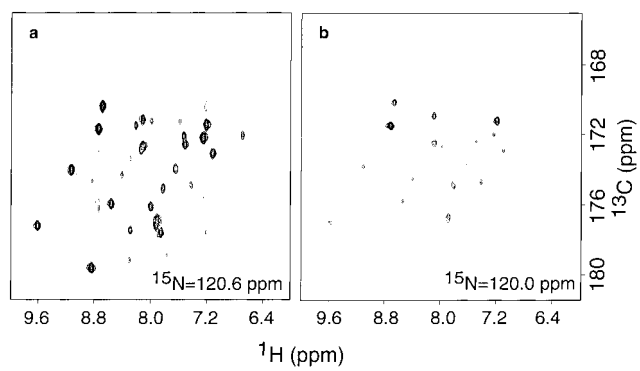

FIG. 2. HNCO spectra of TIM. (a) ^{1}H(F3)/^{13}CO (F1) 2D slice of a TROSY–HNCO spectrum acquired using the pulse sequence in Fig. 1b as described in the text. (b) ^{1}H(F3)/^{13}CO(F1) 2D slice acquired using a conventional gradient-enhanced pulse sequence (*q*).

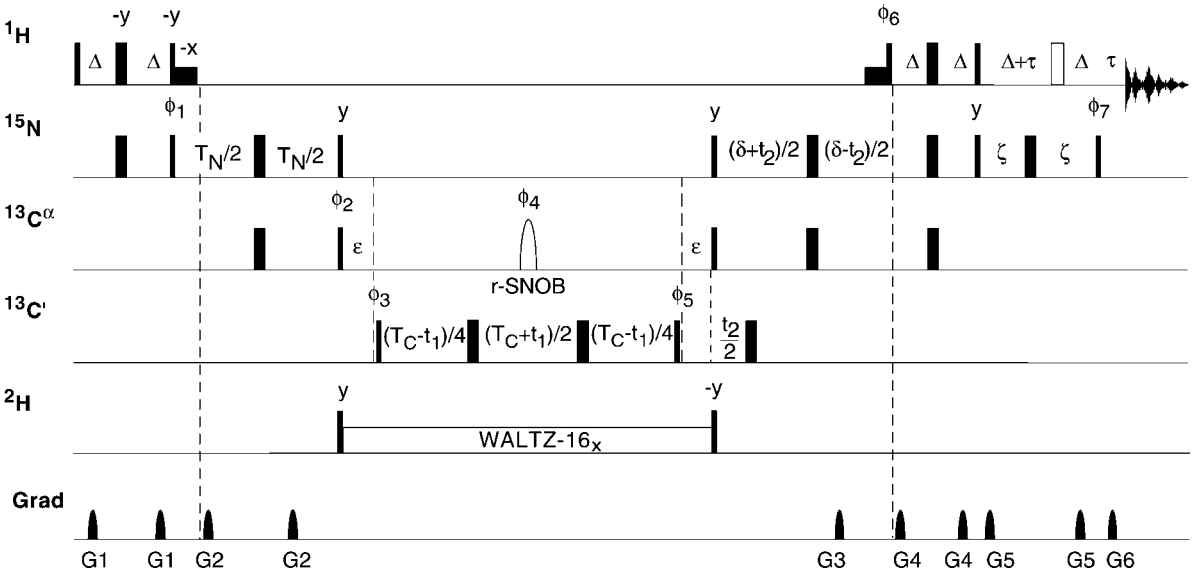

FIG. 3. TROSY–HN(CA)CO pulse sequence. All pulses are applied with *x*-phase unless otherwise indicated. Narrow and wide filled rectangles depict 90° and 180° pulses, respectively and the 3-9-19 composite pulse (*13*) is shown as an open rectangle. The filled squares are low power ^{1}H 90° pulses for water flipback. The proton carrier frequency is set on resonance with the H_2O signal (4.7 ppm), ^{13}CO, $^{13}C_\alpha$, ^{15}N, and ^{2}H carriers are set to 173.0, 55.0, 120.0, and 4.3 ppm, respectively. ^{1}H pulses are applied at $\gamma B_1 = 25$ kHz. All ^{13}C 90° (180°) pulses are applied with a field strength of $\nu/\sqrt{15}$ ($\nu/\sqrt{3}$) where ν is the difference in Hz between the $^{13}C_\alpha$ and ^{13}CO regions of the spectra. $^{13}C_\alpha$ decoupling during ^{13}CO evolution was accomplished with a 180° pulse, that had the r-SNOB profile (*26*), at a field strength of 15.7 kHz and duration of 150 μs. Deuterium decoupling during periods of transverse C_α magnetization is achieved with a WALTZ-16 sequence at a field strength of 2.5 kHz. Delays are $\Delta = 2.75$ ms, $T_N = 22$ ms, $T_C = 14$ ms, and $\epsilon = 7$ ms. The phase cycle is $\phi_1 = 4(x), 4(-x)$; $\phi_2 = x, -x$; $\phi_3 = x, x, -x, -x$; $\phi_4 = 8(x), 8(-x)$; $\phi_5 = 52°$; $\phi_6 = y$; $\phi_7 = x$; receiver $= x, -x, -x, x, -x, x, x, -x$. Gradient pulse lengths and strengths are $G1_z = (520\ \mu s, 6$ G/cm), $G2_z = (600\ \mu s, 4.8$ G/cm), $G3_{xyz} = (1.5$ ms, 24 G/cm), $G4_z = (500\ \mu s, 7.2$ G/cm), $G5_z = (500\ \mu s, 12$ G/cm), $G6_{xyz} = (150\ \mu s, 24.24$ G/cm). The gradient pulses have the shape of the center lobe of a sine function. Quadrature detection in t_1 is achieved by shifting ϕ_3 and the receiver following the States–TPPI protocol (*22*). PEP echo/antiecho coherence selection during t_2 (*23–25*) is obtained by inverting the sign of the gradient G6 and of pulse phases ϕ_6 and ϕ_7. A sensitivity-enhanced, non-gradient-selected version of the pulse sequence is obtained by eliminating G3 and G6, setting $\tau = 0$, and utilizing the sensitivity-enhanced TROSY phase cycle (*14*).

times more sensitive than a conventional PEP–HNCO experiment. Overall, the modified pulse sequence in Fig. 1b is 7–10% more sensitive than the conventional sequence in Fig. 1a; for residues in the active-site loop in TIM, known to undergo chemical exchange linebroadening, the sensitivity gain is greater than 15%.

In TROSY–HNCO (and TROSY–HNCA) experiments, the ^{15}N magnetization can be stored along the *z*-axis during the ^{13}CO ($^{13}C_\alpha$) t_1 evolution period or the ^{15}N coherence can be left in the transverse plane to evolve as ^{15}N–^{13}CO (^{15}N–$^{13}C^\alpha$) multiple quantum coherence during t_1 (*4*). The former approach is implemented in Fig. 1. The latter approach is implemented by eliminating the two 90° ^{15}N pulses surrounding the t_1 period, removing the ^{15}N 180° pulse during t_1, and adjusting the positions of the ^{15}N and ^{13}CO 180° pulses during T and δ to refocus the ^{15}N chemical shift during t_1. The latter strategy allows the entire $T + \delta$ period to be used for frequency labeling. In addition, the 90° water-flipback pulses can be eliminated and water suppression obtained by the approach of Mori and co-workers by adjusting the strengths of G2 and G3 (*12*). The relative sensitivity of the two methods depends on the additional linebroadening due to the transverse ^{15}N coherence during t_1 in the latter compared with the losses due to pulse imperfections in the former. In addition to probe performance, this balance will depend on the size of the protein, the magnetic field employed, and the maximum value of t_1 used. In favorable cases, up to an additional 10% sensitivity can be obtained by leaving the ^{15}N magnetization transverse as multiple quantum coherence during t_1.

The modifications demonstrated for the TROSY–HNCO experiment have proven equally effective in TROSY-based HN(CA)CO, HNCA, HN(CO)CA, HN(CA)CB, and HN(COCA)CB experiments. Figure 3 illustrates a modified version of the TROSY–HN(CA)CO experiment (*5*). This experiment utilizes a constant time period T_C for ^{13}CO evolution that satisfies the relationship $2\epsilon + T_C = 1/J_{CC}$ in which J_{CC} is the $^{13}C_\alpha$–$^{13}C_\beta$ coupling constant (*17, 18*). As a result, mirror image linear prediction can be used to increase resolution in t_1 (*19*) and the $^{13}C_\alpha$–$^{13}C_\beta$ scalar coupling is refocused without the need for selective $^{13}C_\alpha$ pulses (which invariably adversely affect resonances of Gly, Ser, and Thr). The pulse sequence also utilizes a different method of decoupling the passive spins during the ^{15}N evolution period than that illustrated in Fig. 1b. The approach in Fig. 1b enables the entire period δ to be

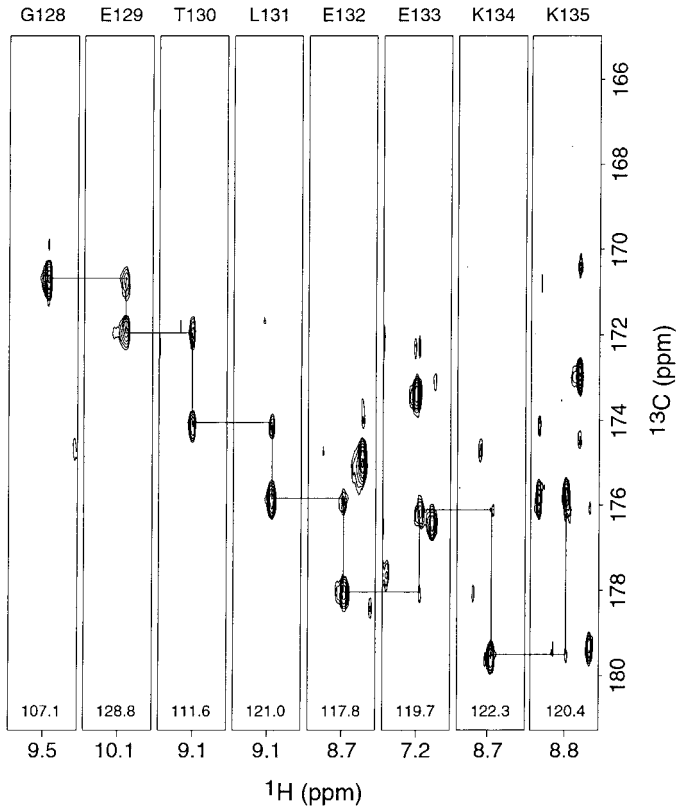

FIG. 4. HN(CA)CO-derived sequential connectivities for TIM. 2D ^{1}H–^{13}CO strips taken from the HN(CA)CO spectra as illustrated for residues 128–135 in TIM. Data were acquired with the pulse sequence shown in Fig. 3 and assignments were confirmed with TROSY HNCO, HNCA, HN(CO)CA, HN(CA)CB, and HN(COCA)CB experiments. The residue name is indicated at the top of each strip along with the ^{15}N chemical shift at the bottom.

utilized for frequency labeling; in the approach illustrated in Fig. 3 the maximum evolution is limited to $\delta - 2(G3 + \tau_{fb})$ in which τ_{fb} is the length of the selective water-flipback pulse. Either approach can be adopted in TROSY triple-resonance experiments. A strip plot of sequential connectivities obtained for the HN(CA)CO experiment is shown in Fig. 4 for TIM. Most importantly, a number of interresidue correlations in TIM were observable only in spectra that utilize the shortened period δ to improve sensitivity.

A final point of interest concerns the effect of ^{13}CO CSA relaxation in triple-resonance spectroscopy of large proteins. The benefits of ^{15}N TROSY-based techniques are greatest at high magnetic field strengths (800–900 MHz) (*1*); however, the ^{13}CO CSA and consequently the ^{13}CO spin–spin relaxation rate constant increases quadratically with field. Most triple-resonance experiments are run in pairs: one experiment uses the $^{1}J_{NC\alpha}$ and $^{2}J_{NC\alpha}$ couplings to correlate the C_{α}^{i} and C_{α}^{i-1} spins to the N^{i} spin and the other experiment uses the $^{1}J_{NCO}$ and $^{1}J_{C\alpha CO}$ couplings to correlate the C_{α}^{i-1} and N^{i} spins (*20*). The latter experiments are very sensitive for small proteins at low magnetic field strengths, but sensitivity decreases as the magnetic field increases and as the size of the molecule increases. As an example, the relative sensitivity of the interresidue correlation in the HN(CO)CA experiment compared with the same correlation in the HNCA experiment is given by

$$S = \frac{\sin^2(\pi J_{NCO}\delta)\sin^2(\pi J_{C\alpha CO}\tau)\exp(-2R_2\tau)}{\cos^2(\pi\,{}^{1}J_{C\alpha N}T)\sin^2(\pi\,{}^{2}J_{C\alpha N}T)}$$
$$\approx 5.4\,\exp(-0.018\ s^{-1}R_2), \qquad [1]$$

in which $\delta \approx 22$ ms, $T \approx 28$ ms, and $\tau \approx 9$ ms, R_2 is the transverse relaxation rate for the ^{13}CO spin, $^{1}J_{NC\alpha} \approx 7$–11 Hz, $^{2}J_{NC\alpha} \approx 4$–9 Hz, $J_{NCO} \approx 15$ Hz, and $J_{C\alpha CO} \approx 55$ Hz. The measured relative sensitivity for HN(CO)CA and HNCA spectra of TIM at 600 MHz is 2.9, which yields an estimate of $R_2 = 27\ s^{-1}$ at 600 MHz. At 900 MHz, the sensitivity of the HN(CO)CA (and other experiments relayed through the ^{13}CO spin) will be less than the HNCA (and other experiments that utilize the $^{2}J_{NC_{\alpha}}$ coupling) for molecules significantly larger than TIM.

A large number of triple-resonance experiments detect the magnetization of protons attached to ^{15}N spins. These pulse sequences invariably include a constant-time period for ^{15}N frequency labeling and refocusing of a ^{15}N–*X* (*X* normally being ^{13}CO or $^{13}C^{\alpha}$ spin) scalar coupling interaction prior to the final reverse polarization transfer period (*20*). These sequences also incorporate water-flipback water suppression for optimal sensitivity (*21*). Thus, the modifications to the HNCO–TROSY pulse sequence presented herein are applicable to any triple-resonance experiment that incorporates a TROSY sequence element for reverse polarization transfer from a ^{15}N spin to a ^{1}H spin.

ACKNOWLEDGMENTS

We thank Clay Bracken (Cornell University) for helpful discussions. Support from Grants GM19247 (J.P.L.), GM40089 (M.R.), and GM59273 (A.G.P.) from the National Institutes of Health are acknowledged gratefully. Acquisition of the DRX600 was made possible by NSF Grant DBI-9601661.

REFERENCES

1. K. Pervushin, R. Riek, G. Wider, and K. Wüthrich, *Proc. Natl. Acad. Sci. U.S.A.* **94,** 12366–12371 (1997).
2. M. Goldman, *J. Magn. Reson.* **60,** 437–452 (1984).
3. K. Pervushin, R. Riek, G. Wider, and K. Wüthrich, *J. Am. Chem. Soc.* **120,** 6394–6400 (1998).
4. M. Salzmann, K. Pervushin, G. Wider, H. Senn, and K. Wüthrich, *Proc. Natl. Acad. Sci. U.S.A.* **95,** 13585–13590 (1998).
5. M. Salzmann, G. Wider, K. Pervushin, H. Senn, and K. Wüthrich, *J. Am. Chem. Soc.* **121,** 844–848 (1999).
6. J. Weigelt, *J. Am. Chem. Soc.* **120,** 12706–12706 (1998).
7. D. Yang and L. E. Kay, *J. Am. Chem. Soc.* **121,** (1999).
8. D. Yang and L. E. Kay, *J. Biomol. NMR* **13,** 3–10 (1999).
9. D. R. Muhandiram and L. E. Kay, *J. Magn. Reson., Ser. B* **103,** 203–216 (1994).

10. M. Czisch and R. Boelens, *J. Magn. Reson.* **134,** 158–160 (1998).

11. S. Mori, C. Abeygunawardana, M. O'Neil Johnson, and P. C. M. van Zijl, *J. Magn. Reson. Ser. B* **108,** 94–98 (1995).

12. A. J. Dingley and S. Grzesiek, *J. Am. Chem. Soc.* **120,** 8293–8297 (1998).

13. V. Sklenar, Piotto, M., Leppik, R. and Saudek, V., *J. Magn. Reson. A* **102,** 241–245 (1993).

14. M. Rance, J. P. Loria, and A. G. Palmer, *J. Magn. Reson.* **136,** 92–101 (1999).

15. J. Cavanagh, A. G. Palmer, P. E. Wright, and M. Rance, *J. Magn. Reson.* **91,** 429–436 (1991).

16. D. Marion, M. Ikura, and A. Bax, *J. Magn. Reson.* **84,** 425–430 (1989).

17. R. Bazzo, D. O. Cicero, and G. Barbato, *J. Magn. Reson., Ser. B* **107,** 189–191 (1995).

18. F. Löhr and H. Rüterjans, *J. Biomol. NMR* **6,** 189–197 (1995).

19. G. Zhu and A. Bax, *J. Magn. Reson.* **90,** 405–410 (1990).

20. J. Cavanagh, W. J. Fairbrother, A. G. Palmer, and N. J. Skelton, "Protein NMR Spectroscopy: Principles and Practice," Academic Press, San Diego (1996).

21. S. Grzesiek and A. Bax, *J. Am. Chem. Soc.* **115,** 12593–12594 (1993).

22. D. Marion, M. Ikura, R. Tschudin, and A. Bax, *J. Magn. Reson.* **85,** 393–399 (1989).

23. A. G. Palmer, J. Cavanagh, P. E. Wright, and M. Rance, *J. Magn. Reson.* **93,** 151–170 (1991).

24. L. E. Kay, P. Keifer, and T. Saarinen, *J. Am. Chem. Soc.* **114,** 10663–10665 (1992).

25. M. Rance, *Bull. Magn. Reson.* **16,** 54–67 (1994).

26. E. Kupce, J. Boyd, and I. D. Campbell, *J. Magn. Reson. B* **106,** 300–303 (1995).